A high resolution whole brain imaging using Oblique Light Sheet Tomography

Arun Narasimhan, Judith Mizrachi, Kannan Umadevi Venkatraju, Dinu F. Albeanu, Pavel Osten

Cold Spring Harbor Laboratory, Cold Spring Harbor, NY 11724.

albeanu@cshl.edu, osten@cshl.edu

Abstract:

We have developed a oblique version of the light sheet microscope to do volumetric imaging of the whole brains at high spatial resolution. Tissue clearing using aqueous techniques reduces the structural rigidity of the brain, To overcome this, we developed a gelatin based re-embedding procedure that makes the brain rigid enough to be sectioned. A few examples of whole brain volumetric images are shown using the oblique light sheet tomography.

Introduction:

Recently, light sheet fluorescence microscopy has become the preferred modality for fast volumetric imaging. It provides the necessary optical sectioning to reduce out-of focus fluorescence, high signal to noise and also speed to image large volumes as the acquisition uses a camera. In a typical design, the light sheet microscope illuminates from the side and the images are acquired perpendicular to the direction of illumination[1]. This design is useful for small samples such as drosophila morphogenesis[2], larval zebrafish[3] monitor, but for larger tissues such as a mouse brain, whose sizes are in a few mm along all directions, the WD of regular high NA objectives limits the imaging field of view.

Current LSFMs are limited in their use with regards to the structural detail they can give. For eg, the Lavision microscope can be used to image at 0.8x magnification (4um pixel size) for the whole brain. This can be used to look at c-fos activation[4] or follow projections of dense bundles[5]. COLM[6], another version of LSFM uses a custom 10x objective to image the samples. This limits the use and observation from the light sheet microscope. A detailed structural analysis of dendritic morphology of the whole brain or axon projection of individual neurons is not possible at this resolution. These require the acquisition to be at higher magnification.

Further, the morphology and density gradient within the tissue (white vs gray matter) modifies the path through which both the excitation and emission photon travels[7]. These changes in the RI of the tissue lead to spherical aberration during imaging and leading to the change in the focal plane of imaging reducing the signal to noise. Even though this has been partially overcome by using modeling this

spherical aberration and deconvolution[8], this requires a apriori knowledge or an iterative calculation of the RI and scattering of the brain at a particular position that depends on density/packing and organization of the cells and varies from structure to structure within the brain. Adaptive optics can be used to correct for these aberrations, but leads to an increase in acquisition time, reducing the advantages of using LSFM as a tool for fast volumetric imaging.

To overcome this we developed a novel light sheet microscope, called the Oblique Light Sheet Tomography (OLST) based on the 'inverted Selective Plane Illumination Configuration' (iSPIM)[9] that uses a high magnification (16x) and also a high NA (0.8). The WD of the objective limits our field of view and to overcome this a vibratome was integrated into the system to serially section the imaged tissue. Since, the illumination is always from the top surface, it reduces/minimizes the tissue scattering related artifacts. The illumination does not have to traverse deep into the tissue, so the beam profile is maintained; further the emission photons are also collected only from this volume of tissue imaged leading to a very high signal to noise. Further, in order to take advantage of frame rate of the camera, we used a continuous motion imaging, with speeds between 0.25mm/s or 0.5mm/s giving us an x-resolution of about 2.5um/frame or 5um/frame.

Many clearing techniques have been developed recently that reduce the tissue scattering by removing the lipid content in the brain, using either an organic [4,10,11] or aqueous based solutions[12,13,14]. Organic solvents, although are the best at removing the lipids and making them transparent, they dehydrate the brain making it very glass like and unfit for sectioning. Also, these clearing processes do not preserve the

native fluorescence of the sample and so require the need to use antibody staining, though boosting the signal to noise ratio, is laborious and time consuming. The use of aqueous clearing techniques relies mostly in the passive diffusion of the solution and the use of detergents, like Triton-X and SDS in CUBIC[13] and CLARITY[12] as the agents to remove the lipids. This increases the incubation time, but the structural integrity of the brain is maintained as well the fluorescence from the various fluorescent proteins.

Here, we modified the CUBIC (mCUBIC) based aqueous clearing protocol, to preserve the native fluorescence and to make the brain structurally rigid. Clearing essentially removes the phospholipids from the tissue. This makes the tissue structurally weaker and soft and difficult to handle for sectioning. To make the brain rigid enough to section, we developed a novel gelatin based hydrogel embedding protocol. This gelatin-based hydrogel embedding protocol makes the brain more rigid than the acrylamide based hydrogel (CLARITY, PARS/PACT) and thus can be used for sectioning purposes.

Materials and methods:

Clearing:

The clearing protocol was altered from the original CUBIC protocol[13]. One of the components, urea from the original Scale/CUBIC-1 solution was removed and this solution was used as the clearing solution, named mCUBIC (modified CUBIC). The clearing protocol followed the steps similar to the original CUBIC protocol. The brain was immersed in the mCUBIC solution and was incubated in a shaker oven at 37°C. 4 days later the solution was changed and the brain was incubated at 37°C in a shaker oven. 1 week after clearing, the brain was then washed three times using 0.05M PB solution and stored at RT. After 12 hrs of incubation at PB solution, the brain was again washed three times in PB solution and stored in 4°C fridge overnight. The following day, the brain was again washed 3 times using the PB solution. This process of repeated washing removed the clearing solution from the brain.

A 5% gelatin solution in PB containing 0.01% of Sodium Azide was prepared and the solution was heated in an incubator oven at 42°C for two hrs to solubilize the gelatin[16,17]. Now, the gelatin solution was cooled to 37°C and the cleared brain put into it and allowed to soak the gelatin. After 1 hr, only the brain was removed from the gelatin solution and cooled to RT for 15 mins. Now, this gelatin embedded brain was then incubated in 4% PFA solution overnight at 4°C. This helped crosslink the gelatin and make the brain structurally rigid, so that it can be sectioned using the standard vibratome. The brain was then washed in PB solution to remove excess PFA.

Microscope:

The OLST uses two water-dipping objectives, in the 'inverted selective plane illumination microscopy (iSPIM)' configuration, that are non-symmetric. A laser (488nm or 561nm, Coherent) was expanded to 2.6mm using a beam expander and a pin-hole, onto a galvanometer scan mirror, which generated the light sheet by digital scanning, and was imaged onto the back focal plane of a low numerical aperture (NA) illumination (Nikon PlanFluor 10x, 0.3 NA, wd = 3.5mm, water) objective, representing a NA of 0.065 that was used.

The fluorescence was then collected using a high NA objective (Nikon LWD 16x, 0.8 NA, 3mm WD, water) coupled to a tube lens that projected the image onto a sCMOS (Andor Zyla 4.2) camera giving us a pixel size of 0.406μm along x and y of the detection arm. We typically readout from only half the chip of the camera so that fluorescence collected is essentially from the central part of the Gaussian light sheet, giving us a very high axial resolution, giving us a FOV of 832*416μm along the detection axis. The spherical aberration due to the RI mismatch (water 1.33 to clearing solution 1.42 to the gelatin embedded tissue-1.48) is taken care during alignment.

We follow the reference co-ordinate system as mentioned in [15]. Briefly, the tissue is in the x',y' and z' reference co-ordinate with z=0 being the top surface of the tissue, x, y and z the microscope reference coordinates, with z being the detection objective's optical axis. In a typical experiment, to acquire images at the maximum readout rate of the camera (280MHz), 100fps, we moved the sample continuously at

0.5mm/s or 0.25mm/s, to give us a 5 or 2.5μm along x' and 2000 or 4000 frames to give us a volume of 10000*832*294μm along x', y' and z'.

The sample is then translated 800μm along y' and then the next stack is acquired. This process is repeated until the mouse brain is imaged from side to side. After which the sample was translated to the integrated vibratome to section out the tissue volume that has been imaged. The typical z-section thickness is about 250μm along z' corresponding to 355μm along y of the detection arm, while we image 416μm. This gives us an overlap of about 60μm along z or about 44μm along z' to register the corresponding sections.

A custom written software program was used for both the acquisition in LabView and reconstruction in MATLAB. The oblique images were sheared and transformed into coronal images for viewing and registration purpose in MATLAB, while all the analysis was done using the raw obliquely acquired images.

Prior to imaging, the brain was then incubated in clearing solution for 12hrs at 37°C. This allowed the clearing solution to penetrate and make the brain translucent again. The brain is then embedded in agarose, which is further crosslinked using the sodium borate buffer for 3 hrs, and then imaged in OLST.

Results:

A 750μm section of the brain was cleared in 3 hrs, while the whole brain was cleared in 1 week. The brain was incubated in mCUBIC solution for 1 week, where the solution was changed once after 4 days. After 1 week, the brain increases in size due to hyperhydration (fig. 1.b) from the clearing solution. Now, the brain is then embedded in 5% gelatin matrix (fig 1.b). Now, this embedded brain is then incubated overnight in the clearing solution before imaging in our custom built light sheet microscope (OLST).

The light sheet is in the 'inverted Selective Plane Illumination Microscopy (iSPIM)' configuration (Fig. 1.c). This oblique orientation allows for imaging the surface of the brain (oblique depth ≈400 μm) in an XY raster pattern. Once the raster scan is completed, the brain is moved to an integrated vibratome to section the imaged top 250μm tissue. This sequence of raster scan (Fig 1.d) and automated sectioning is repeated to obtain fluorescence image of the whole brain. We imaged only one half of the sCMOS sensor (Andor Zyla 4.2) so as to be in the narrow portion of the light sheet to reduce the out-of-focus fluorescence signals. The illumination parameters are 100μm width and 5μm thickness at the center of the beam. The PSF of the microscope is 0.65*0.65μm along x and y, which is slightly greater than the actual pixel width (0.406μm), while along the z-direction the laser is about 6.5μm wide at the beam waist.

The oblique geometry gives us a distinct advantage with the imaging plane always being from surface to the depth inside the tissue that is limited by the camera FOV. To show that we can have homogenous illumination, we imaged a perfused 8-week

old GAD-H2B-GFP mouse brain that was processed using mCUBIC protocol, using OLST. Fig 2a, b, c show the low resolution volumetric rendering, a horizontal cross section and sagittal rendering of the imaged brain. Fig2d shows a high-resolution optical section from the striatal region of the mouse brain. Individual cells were detected even when such dense labeling is present as seen in Fig 2e and f. The whole brain of the mouse was imaged in 8 hrs at 0.4*0.4*5μm resolution. The geometry of oblique illumination with the imaging from surface to a depth that is always constant gives rise to uniform detection parameters without any spherical aberrations.

An important part of neuroanatomy is to reconstruct the morphology of neurons. This gives us an idea of the flow of information within the brain. In order to reconstruct the morphology of neurons, a Thy1-GFP mouse brain was imaged using the OLST. We used a 2.5μm x-step to reduce the motion artifacts and to see detailed morphology from whole brain. The whole brain was imaged in 14hrs to produce a raw data of about 11TB. Fig 3 shows the whole brain image of a Thy1-GFP mouse imaged. We can see spines in the along the whole brain (Fig 3d and f). OLST is the first microscope where we can see whole brain at spine level resolution.

Conclusions:

We have developed a robust light sheet fluorescence microscope, in the oblique geometry, that can image whole tissues at high resolution. It combines the advantages of fast imaging using a camera and serial sectioning to maintain an uniform illumination profile. Since, scattering limits the penetration depth of the incident photons, we adapted and modified the CUBIC clearing protocol to clear the sample and then to embed it in gelatin to make it rigid enough to be sectioned using the integrated microtome. In summary, we have developed a combination of clearing, embedding the cleared brain to make it rigid enough to section, and an oblique light sheet fluorescence microscope with a high spatial resolution to see the dendritic morphology and also trace axons along the whole brain.

Figure Captions:

Figure 1. (a) A 750um section before and after clearing using the mCUBIC protocol. (b) mCUBIC clearing protocol and timeline – a fixed brain incubated in clearing solution at 37°C, after 4 days the solution is changed. After 1 week, the clearing is stopped and the brain is washed PB. The following day, the brain is embedded in 5% gelatin matrix to make it rigid enough to be sectioned by a microtome. Prior to imaging, the gelatin embedded brain is incubated in clearing solution (37°C) to make the brain translucent. (c) Oblique Light Sheet Tomography schematic consisting of the 10x illumination objective and the 16x detection objective and the vibratome integrated into the setup. (d) Reconstruction pipeline of the images acquired by OLST.

Figure 2. (a) Low resolution volume rendering of the GADH2B-GFP whole brain (b) Horizontal and (c) Sagittal sections from the whole brain. (d) A representative coronal section from the GADH2B-GFP. Scale bar - 2mm. (e) striatum and (f) cortical zoom in view from the same section illustrating the high signal to noise. Scale bar – 50μm.

Figure 3. (a) and (b) Sagittal and Horizontal rendering of a Thy1-GFP brain imaged using OLST. Scale bar – 2mm. (c) and (e) Coronal images at two different regions of the brain – (c) anterior and (e) posterior. Scale bar – 2mm. (d) and (f) High resolution images from the coronal images showing spines. Scale bar – 25μm.

References:

1. Huisken, J. Optical Sectioning Deep Inside Live Embryos by Selective Plane Illumination Microscopy. *Science* **305,** 1007–1009 (2004).
2. Keller, P. J., Schmidt, A. D., Wittbrodt, J. & Stelzer, E. H. Reconstruction of zebrafish early embryonic development by scanned light sheet microscopy. *Science* **322,** 1065–1069 (2008).
3. Ahrens, M. B., Orger, M. B., Robson, D. N., Li, J. M. & Keller, P. J. Whole-brain functional imaging at cellular resolution using light-sheet microscopy. *Nature Methods* **10,** 413–420 (2013).
4. Renier, N. *et al.* Mapping of Brain Activity by Automated Volume Analysis of Immediate Early Genes. *Cell* **165,** 1789–1802 (2016).
5. Ye, L. *et al.* Wiring and Molecular Features of Prefrontal Ensembles Representing Distinct Experiences. *Cell* **165,** 1776–1788 (2016).
6. Tomer, R., Ye, L., Hsueh, B. & Deisseroth, K. Advanced CLARITY for rapid and high-resolution imaging of intact tissues. *Nature Protocols* **9,** 1682–1697 (2014).
7. Lichtman, J. W. & Conchello, J. A. Fluorescence microscopy. *Nature Methods* (2005).
8. Tomer, R. *et al.* SPED Light Sheet Microscopy: Fast Mapping of Biological System Structure and Function. *Cell* **163,** 1796–1806 (2015).
9. Wu, Y. *et al.* Inverted selective plane illumination microscopy (iSPIM) enables coupled cell identity lineaging and neurodevelopmental imaging in Caenorhabditis elegans. *Proc. Natl. Acad. Sci. U.S.A.* **108,** 17708–17713 (2011).

10. Renier, N. *et al.* iDISCO: a simple, rapid method to immunolabel large tissue samples for volume imaging. *Cell* **159,** 896–910 (2014).

11. rk, A. E. U. *et al.* Three-dimensional imaging of the unsectioned adult spinal cord to assess axon regeneration and glial responses after injury. *Nature Medicine* **18,** 166–171 (2011).

12. Chung, K. *et al.* Structural and molecular interrogation of intact biological systems. *Nature* (2013). doi:10.1038/nature12107

13. Susaki, E. A. *et al.* Whole-brain imaging with single-cell resolution using chemical cocktails and computational analysis. *Cell* **157,** 726–739 (2014).

14. Susaki, E. A. *et al.* Advanced CUBIC protocols for whole-brain and whole-body clearing and imaging. *Nature Protocols* **10,** 1709–1727 (2015).

15. Nylk, J., McCluskey, K., Aggarwal, S., Tello, J. A. & Dholakia, K. Enhancement of image quality and imaging depth with Airy light-sheet microscopy in cleared and non-cleared neural tissue. *Biomed Opt Express* **7,** 4021–4033 (2016).

16. Nagamoto-Combs, K., Manocha, G. D., Puig, K. & Combs, C. K. An improved approach to align and embed multiple brain samples in a gelatin-based matrix for simultaneous histological processing. *J. Neurosci. Methods* **261,** 155–160 (2016).

17. Economo, M. N. *et al.* A platform for brain-wide imaging and reconstruction of individual neurons. *Elife* **5,** e10566 (2016).

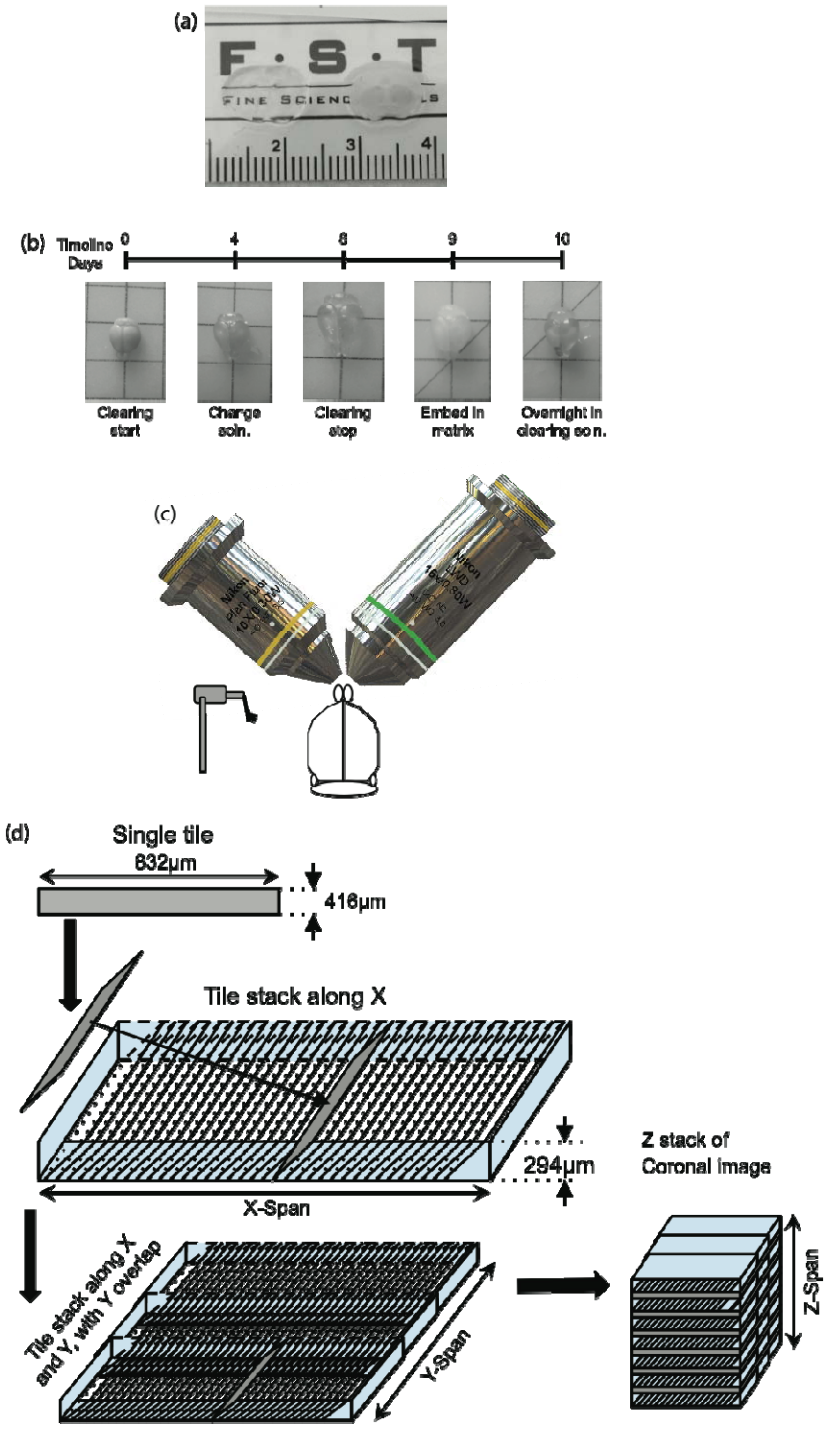
(a)
F · S · T
FINE SCIENC
(b)
Timeline
Days
0
4
8
9
10
Clearing start
Charge soln.
Clearing stop
Embed in matrix
Overnight in clearing soln.
(c)
(d)
Single tile
832µm
416µm
Tile stack along X
294µm
X-Span
Z stack of
Coronal image
Tile stack along X and Y, with Y overlap
Y-Span
Z-Span

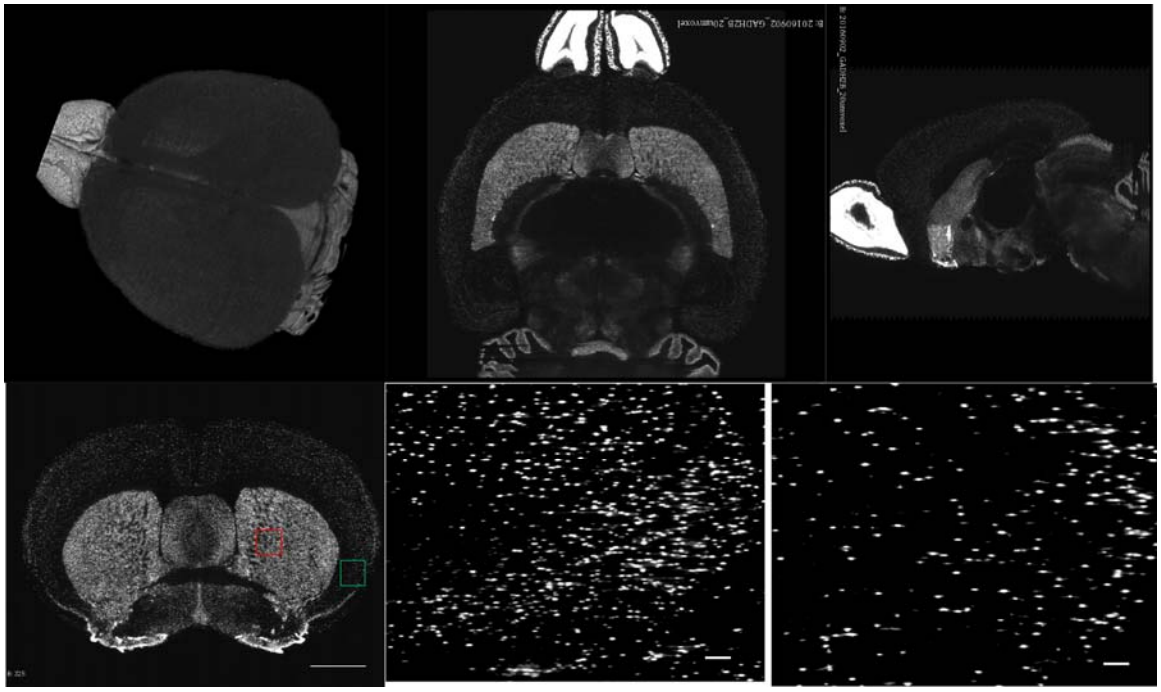

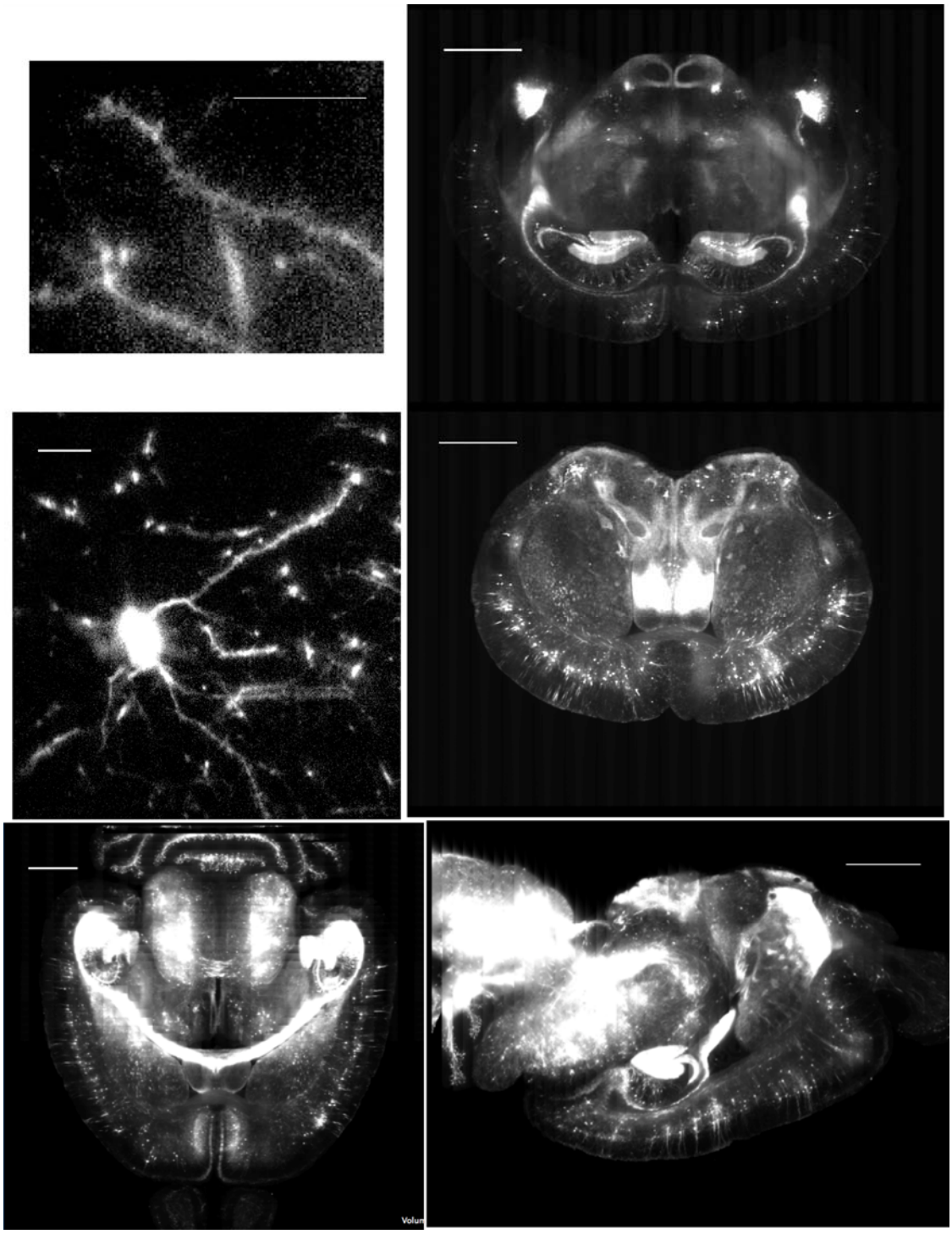
Volum